Current Biology, Volume *23*

Supplemental Information

Polyploidization and Cell Fusion Contribute to Wound Healing in the Adult *Drosophila* Epithelium

Vicki P. Losick, Donald T. Fox, and Allan C. Spradling

Inventory of Supplemental Information

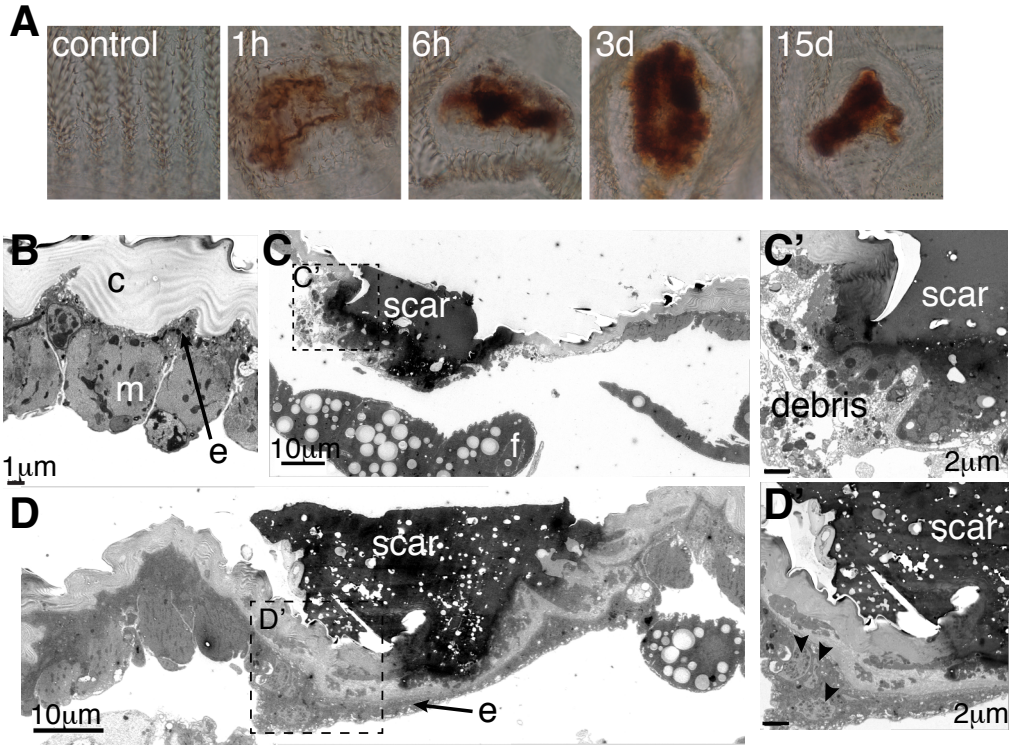

Figure S1. Scar formation and ultrastructural analysis of wound healing, related to Figure 1. (A) Micrographs of the Drosophila cuticle. Melanin accumulated at wound site forming a scab at the indicated time post injury. (B-D) Electron micrograph images of (B) Control, uninjured tissue organization. Cuticle (c), muscle fiber (m), and epithelium (e, arrow) are marked. (C) At 1 day post injury both muscle and epithelium have retracted from the injury site and only debris is present below the scar (C'). Overlaying fat body (f) is in loose contact with abdominal tissue. (D) 2 days post injury epithelium reseals below scar and a cluster of epithelial nuclei are present at wound edge (D', arrowheads).

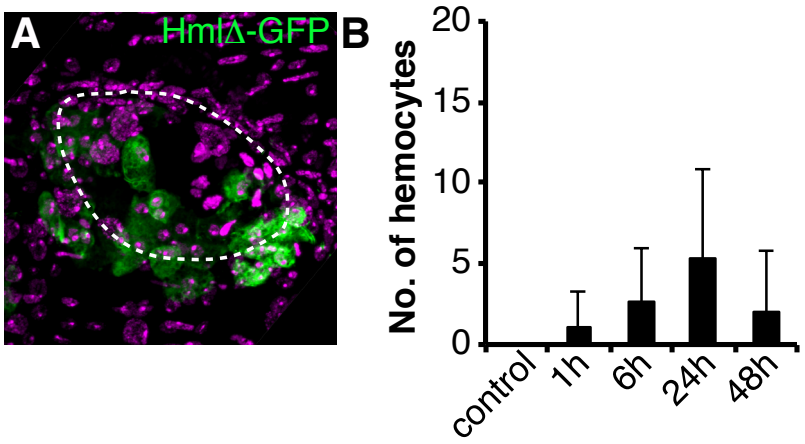

Figure S2. Hemocytes are recruited to wound site when cells re-enter S phase, related to Figure 1. (A) Immunofluorescent image of hemocytes accumulating at the wound site by 1 day post injury. HmlΔ-Gal4, UAS-EGFP marks hemocytes (green). DAPI (magenta). Scar (dashed white line). (B) Average number of hemocytes recruited to wound site at the indicated time (N=10-50, mean +/- SD).

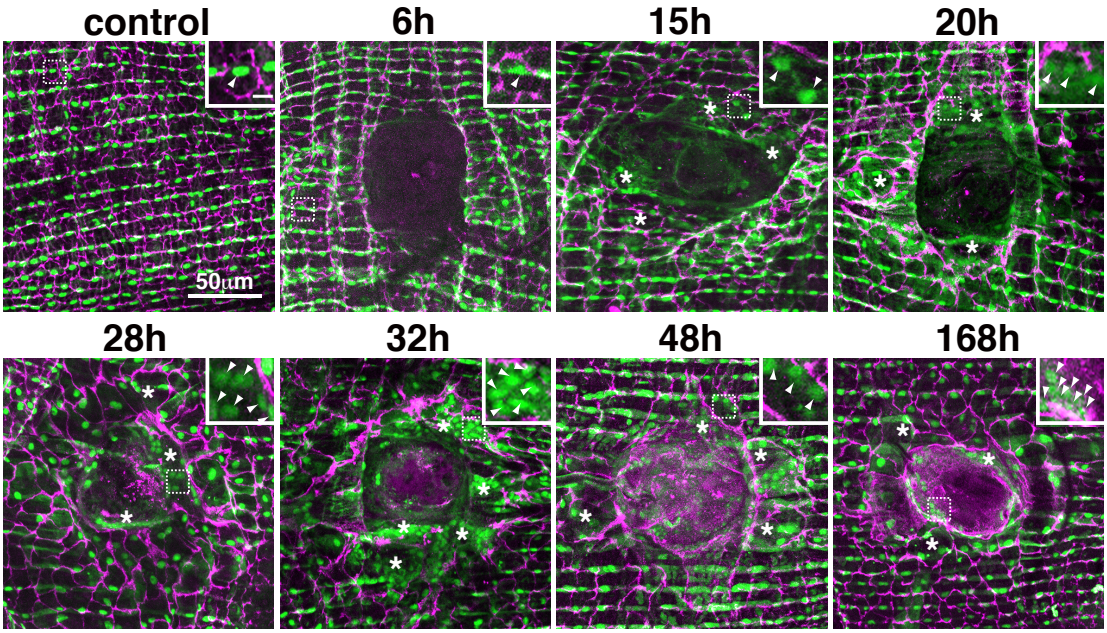

Figure S3. Re-epithelialization time course, related to Figure 3. Immunofluorescent images taken at indicated time post injury during resealing of the epithelium. Epithelial nuclei (green, flpout nlsGFP; Epithelial-Gal4/ UAS-Flp) and FasIII (magenta). Sites of cell fusion are marked with asterisk (*) and examples are boxed and shown in the figure's inset with arrowheads pointing to the epithelial nuclei.

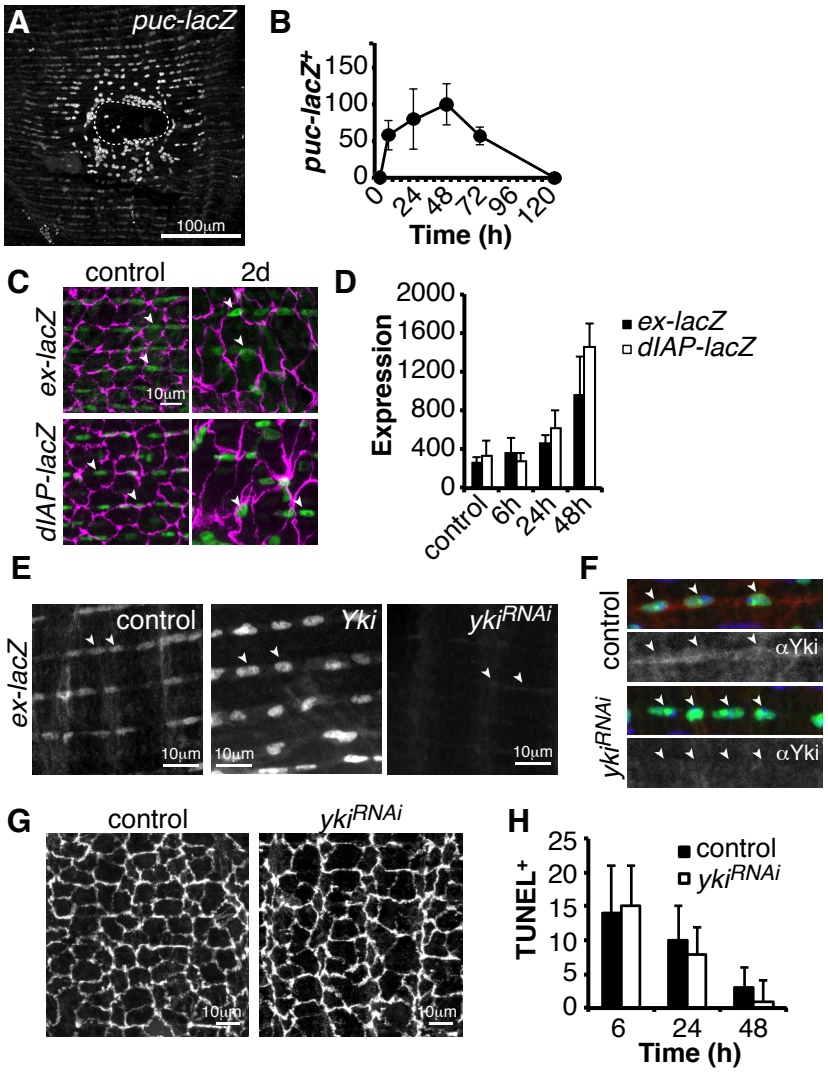

Figure S4. JNK and Hippo pathway regulation, related to Figure 5. (A-D) JNK and Hippo regulated gene expression is activated by injury. (A) Immunofluorescent image of JNK reporter (*puc-lacZ*) at 1 day post injury. (B) Time course of *puc-lacZ* activation (N=5-10 wounds, mean +/- SD). (C) Immunofluorescent images of Yki reporter activation, shown are *ex-lacZ* and *dIAP-lacZ*. β–gal (green) and FasIII (magenta). (D) Expression of *ex-lacZ* and *dIAP-lacZ* (N=90, mean +/- SD). (E-F) Knocking down *yki* efficiently blocks Yki controlled gene expression and Yki protein. (E) Immunofluorescent images of *ex-lacZ* expression in control (without a transgene) or with the indicated UAS-transgene driven by Epithelial-Gal4. (F) Immunofluorescent images of Yki protein expression in control or with Epithelial-Gal4/ UAS-$yki^{RNAi\#2}$. Epithelial nuclei (green, flpout nlsGFP; Epithelial-Gal4/ UAS-Flp). αYki (red). DAPI (blue). (G) Cell fusion is not affected in uninjured yki^{RNAi} expressing flies. Immunofluorescent images of FasIII organization in control and Epithelial-Gal4/ UAS-$yki^{RNAi\#2}$. (H) TUNEL assay with control and Epithelial-Gal4/ UAS-$yki^{RNAi\#2}$ (N=10 wounds, mean +/- SD). Arrowheads mark sample nuclei.

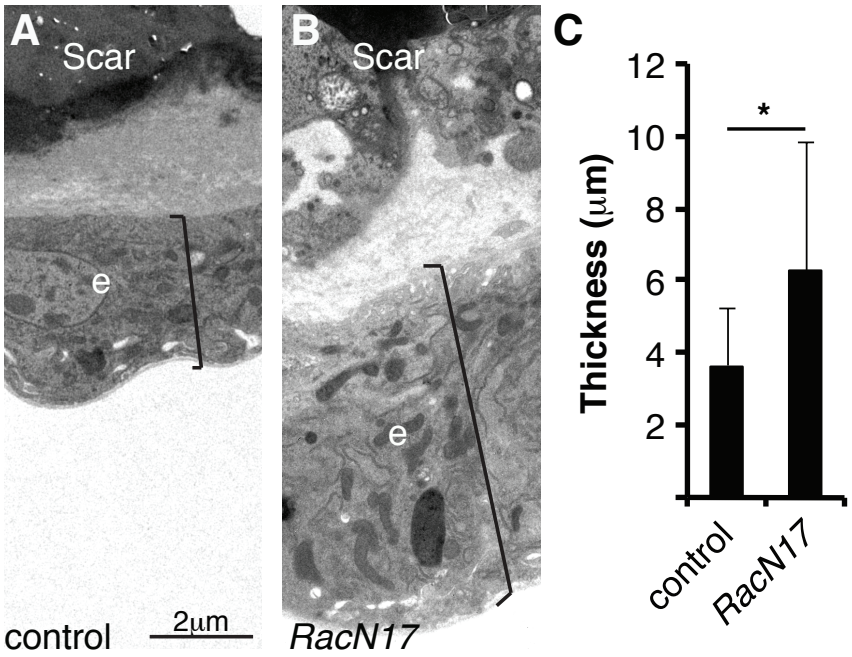

Figure S5. Blocking cell fusion enhances epithelial thickness under the scar, related to Figure 6. Representative electron micrograph images from regions under the scar at 3 days post injury in (A) control (Epithelial-Gal4 alone) and (B) Epithelial-Gal4/ UAS-*RacN17* flies. Epithelium (e). Brackets mark regions measured. (C) Quantification of epithelial thickness (N=30, mean +/- SD). (*) T-test, p= 0.05.

Movie S1. Repaired epithelium cups the scar, related to Figure 3. A 3D reconstruction of a immunofluorescent image of a healed wound at 7 days post injury. Epithelial nuclei (green, flpout nlsGFP; Epithelial-Gal4/ UAS-Flp); FasIII (red); pseudo colored scar, (gray).

Supplemental Experimental Procedures

Fly strains and reagents

Additional fly strains used in this study were from Bloomington, VDRC, or fly community as indicated. UAS-Flp (Bloomington #4539); *ex-lacZ* (Bloomington #11067); *dIAP-lacZ* (Bloomington #12093); *puc-lacZ* (Bloomington #11173); UAS-$cycE^{RNAi}$ (#1= Bloomington #29314, #2= VDRC #110204); UAS-$E2F^{RNAi}$ (VDRC #108837), UAS-yki^{RNAi} (#1= Bloomington #31965, #2= Bloomington #34067), UAS-*tubulin*-GFP (Bloomington); UAS-mCD8-ChRFP (Bloomington #27392); UAS-*RacN17* (Bloomington #6292); HmlΔGal4, UAS-2xEGFP (Bloomington #30140); UAS-*Hpo* [S1]; PCNA-GFP [S2]; GFP-Polo [S3]; $CycB^{CC01846}$(Carnegie Protein Trap);

Wounding assay and dissection

Three to seven days old adult female flies were punctured once one either side of the ventral midline between tergites A2 and A6 with a 6μm diameter sharpened tungsten needle (Small parts). At indicated times abdomens were dissected in Grace's insect cell medium (Invitrogen) at room temperature under a light dissecting microscope. The internal organs were removed and the abdomens were filleted open by cutting along the dorsal midline with dissecting Vannas spring scissor (Fine Science Tools, #15000-00). Filleted abdomens were pinned down on a Slygard plate with 10μm insect needles. Attached fat body was gently removed with dissecting forceps, if necessary. Based on the extent of the injury and the response of epithelial cells to this procedure, all subsequent quantitative assays focused on an area of about 7.5 $x10^4$ μm^2 centered on the wound, which we found was sufficient to include all the cells responding to the wound, i.e. about 100μm from the wound edge plus a small margin.

Immunostaining and microscopy

Abdomens were fixed in 3.7% formaldehyde in 1x PBS for 30 minutes at room temperature. Primary antibodies were used overnight at 4^0C. Antibodies and dilutions used in this study are rabbit anti-GFP (Invitrogen, 1:2000), mouse anti-FasIII (DSHB, 1:50), chicken anti-βgal (Abcam, pre-absorbed, 1:1000), rabbit anti- Phospho H3 (Cell Signaling, 1:100), rabbit anti-Yki (1:500) [S1] and rabbit anti-Grh (1:300) [S4]. Secondary antibodies from Invitrogen included donkey anti-rabbit 488, goat anti-rat 568, and goat anti-chicken 488 (1:500). Alexa Fluor 633 Phalloidin (Invitrogen, A22284). Stained abdomens were mounted in vectashield on glass coverslip, with the inside tissue facing out. Images were taken on Sp5 confocal microscope or ZEISS ApoTome and processed with ImageJ software to compile into a z-stack projection. Image brightness and contrast was adjusted linearly with Adobe Photoshop software.

EdU labeling
Flies were fed 75µl of 5mM EdU yeast slurry 2 days prior to injury and continued until dissection. EdU was detected according to manufactures instructions (Click-it EdU Imaging Kit, Invitrogen).

Wound closure assay
Wound closure was measured by scoring for the positive formation of a continuous epithelial sheet under the melanin scab. Gal4/ UAS system was used to express cytoplasmic (tub-GFP) or membrane bound (CD8-RFP) to detect the adult abdominal epidermis. Only abdomens without processing perturbation were analyzed and at least 10 wounds per time point were scored.

Cell size measurements
Changes in cell size and shape were analyzed within the standard 7.5 $x10^4$ μm^2 region surrounding each wound. FasIII boundaries were analyzed from compiled Z- stack projections in ImageJ software. Cell area was measured and number of epithelial nuclei per boundary was recorded for at least 50 cells per image with 2-5 abdomens scored per condition.

Ploidy measurements
Changes in DNA content were analyzed within the standard 7.5 $x10^4$ μm^2 region surrounding each wound. Female abdomens from indicated genotype and testis from oreR flies were dissected in 0.7% NaCl at room temperate. Tissue was treated with 0.5% NaCitrate for 10 minutes and then fixed for 30 minutes in 4% paraformaldehyde in 1x PBS. Tissue was squashed in vice on a coated coverslip and them submerge in liquid nitrogen to remove coverslip. Tissues were dehydrated in 100% EtOH 15 minutes and washed with 1xPBS. Slides were stained with DAPI (1:5000) for 15 minutes, washed, and allowed to dry before mounting. Samples were imaged using an Sp5 confocal microscope with a 40× oil immersion objective. Testis within each slides were image at same gain and settings. The spermatids were used as an internal control for ploidy measurements. Images were analyzed using ImageJ. Regions were drawn around each nucleus using the trace function and integrated fluorescence intensity was measured within each region. Background for each nucleus was calculated and subtracted from the average intensity. The average DAPI intensity of sperm cells (1c) on same slide were analyzed and calculated. The theoretical average intensities were calculated on the basis of the measured 1c spermatids. Average intensity values were binned into the groups: 2c (1.0-3.4), 4c (3.5-6.4), and 8c (6.5-14). At least 50 nuclei were counted per image and 3 abdomens were scored for each condition.

Electron microscopy
Female abdomens were dissected as described early, but reagents were kept cold during dissection and fixation. One side of ventral abdomen was trimmed down after it was fixed for 10 minutes on ice in 3% gluteraldehyde, 1% formaldehyde, 0.1 M cacodylate buffer, 2 mM Ca + Mg (pH 7.4). After trimming the abdomens were fixed for additional hour at 4^0C, embedded in agarose at ~50°C, and washed three times for 5 minutes in cacodylate buffer. They were then rinsed for 5 minutes in 0.05 M maleate (pH 6.5), 0.75

hours in 1%OsO4 in cacodylate buffer, and incubated for 1.5 hours in 0.5% uranyl acetate, 0.05 M maleate. After rinsing in H_2O, they were put through a graded ethanol dehydration series and epoxy embedding. Abdomens were cut on a Leica Ultracut S then stained with Pb citrate. Images were captured with a Phillips Tecnai 12 microscope and recorded with a GATAN multiscan CCD camera using Digital Micrograph software.

Hindgut experiments

Hindgut tissue damage was administered genetically as described in [S5]. For acute injury/recovery experiments, flies were placed at 29^0C for 24 hours, and then shifted to 18 degrees for 1-2 weeks. Antibody staining was as in [S5]. Ploidy analysis was done as in [S6]. Huygens deconvolution software was used to analyze DE-Cadherin localization in the hindgut.

Supplemental References

S1. Dong, J., Feldmann, G., Huang, J., Wu, S., Zhang, N., Comerford, S.A., Gayyed, M.F., Anders, R.A., Maitra, A., and Pan, D. (2007). Elucidation of a universal size-control mechanism in Drosophila and mammals. Cell *130*,1120-33.

S2. Thacker, S.A., Bonnette, P.C., and Duronio, R.J. (2003). The contribution of E2F-regulated transcription to Drosophila PCNA gene function. Curr Biol *13*, 53-8.

S3. Royou, A., Gagou, M.E., Karess, R., and Sullivan, W. (2010). BubR1- and Polo-coated DNA tethers facilitate poleward segregation of acentric chromatids. Cell *140*, 235-45.

S4. Kim, M., and McGinnis, W. (2011). Phosphorylation of Grainy head by ERK is essential for wound-dependent regeneration but not for development of an epidermal barrier. Proc Natl Acad Sci U S A 108, 650-5.

S5. Fox, D.T., and Spradling, A.C. (2009). The Drosophila hindgut lacks constitutively active adult stem cells but proliferates in response to tissue damage. Cell Stem Cell *5*, 290-297.

S6. Fox, D.T., Gall, J.G., and Spradling, A.C. (2010). Error-prone polyploid mitosis during normal Drosophila development. Genes Dev *24*, 2294-2302.